

Dedicated to the memory of Prof. dr. Ioan Silaghi-Dumitrescu marking 60 years from his birth

SPECTROSCOPIC AND STRUCTURAL CHARACTERISATION OF $\text{SiO}_2\text{-Y}_2\text{O}_3$ BASED MATERIALS WITH LUMINESCENT PROPERTIES

LAURA ELENA MURESAN^{a,*}, ELISABETH-JEANNE POPOVICI^a,
ECATERINA BICA^a, ADRIAN-IONUŢ CADIŞ^a,
MARIUS MORAR^a AND EMIL INDREA^b

ABSTRACT. Cerium activated yttrium silicate phosphors show blue luminescence under UV excitation. Phosphor utilisation depends on powder characteristics and luminescence properties that are regulated during the synthesis stage. In this paper yttrium silicate based phosphors were prepared by solid state reaction using different molar ratio between SiO_2 and Y_2O_3 . The effect of chemical composition and structure on luminescent properties of phosphors were investigated and discussed.

Keywords: *yttrium silicate, luminescence, solid state reaction*

INTRODUCTION

Yttrium silicate phosphors (Y_2SiO_5) doped with Eu^{3+} , Ce^{3+} , Pr^{3+} , Tb^{3+} or Yb^{3+} are well known luminescent materials due to their luminescent characteristics [1]. Under UV excitation $\text{Y}_2\text{SiO}_5\text{:Ce}$ phosphor exhibits blue-white emission with the peak maximum situated at 414 nm.

Y_2SiO_5 phosphor is usually used as luminescent material in fluorescent lamps, field emission display (FED) and projection television (PTV) because of its brightness, acceptable atmospheric stability and quantum efficiency [2,3].

Many methods such as solid state reaction, sol gel techniques, spray pyrolysis and combustion synthesis have been used to prepare silicate phosphors [4-6]. The analysis of the $\text{Y}_2\text{O}_3\text{-SiO}_2$ phase diagram shows the presence of various compounds such as: Y_2O_3 , SiO_2 , Y_2SiO_5 and $\text{Y}_2\text{Si}_2\text{O}_7$, depending on the synthesis temperature [7,8].

In correspondence to the 1:1 molar ratio, we can find two type of monoclinic Y_2SiO_5 ($\text{Y}_2\text{O}_3\cdot\text{SiO}_2$), known as X1- Y_2SiO_5 phase (crystallographic group P21/c) and X2- Y_2SiO_5 phase (crystallographic group B2/b) [9,10]. The

^a Raluca Ripan Institute for Research in Chemistry, Babes Bolyai University, 400294, Cluj-Napoca, Romania, * laura_muresan2003@yahoo.com

^b National Institute for R &D of Isotopic and Molecular Technologies, 400295 Cluj-Napoca, Romania

second compound in the system is $Y_2Si_2O_7$ ($Y_2O_3 \cdot 2SiO_2$), which shows an even more complex polymorphism, since six $Y_2Si_2O_7$ different structures are reported for it [11].

In practical applications the chemical reaction between rare earth oxides and silicon dioxide at elevated temperatures should be considered as a possible cause of drastic modification of both structure and luminescent properties of yttrium silicate-based powders.

In this paper yttrium silicate phosphor samples were prepared by solid state reaction using different molar ratios between SiO_2 and Y_2O_3 . The effect of chemical composition and structure on optical properties of Ce^{3+} activated yttrium based silicates were investigated and discussed. Samples were characterised by infrared absorption spectroscopy (FT-IR), X-ray diffraction (XRD), and photoluminescence spectroscopy, i.e. emission (PL) and excitation (PLE) spectra.

RESULTS AND DISCUSSION

The Y_2O_3 - SiO_2 phase diagram is currently explored with a variety of synthesis techniques especially in the 1:1 and 1:2 molar ratio domains because of the optical properties that can be induced by dispersion of rare-earth elements such as Eu^{3+} , Tb^{3+} and Ce^{3+} into the matrix. According to the diagram phase [8] several compounds can be detected depending on the Y_2O_3 - SiO_2 molar ratio.

In order to study the influence of the powders composition on the structure and luminescent properties, yttrium silicate based materials were prepared by solid state reaction route at $1400^\circ C$ using different $SiO_2:Y_2O_3$ molar ratios ($MR_{Si:Y}$) namely: 1:4 (sample code YSO25); 1:1 (sample code YSO26); 1:0.5 (sample code YSO27) and 1:0.25 (sample code YSO28). The photoluminescence of the samples YSO29, YSO30, YSO31 and YSO32 was induced by adding 3% mol $Ce/(Y+Ce)$ in the mixture of silicon dioxide and yttrium oxide.

The crystalline structure and structural homogeneity of the powders were put in evidence by XRD measurements (Figure 1).

The XRD patterns indicate that all the powders contain mainly crystalline phases. Also, the XRD patterns confirm the structural changes that occur due to the addition of various amounts of SiO_2 in the synthesis mixture. Different compounds such as: $X1-Y_2SiO_5$ (low temperature phase); $X2-Y_2SiO_5$ (high temperature phase) and monoclinic $Y_2Si_2O_7$ together with unreacted Y_2O_3 and SiO_2 can be identified. It can be also observed that the increase of SiO_2 amount in the synthesis mixture determines changes in both, the composition and structure.

Based on the XRD patterns, the unit cell parameters and the quantitative phase composition were determined through Rietveld refinement using the PowderCell software. The amount (volume percentage) of the various phases in the silicate based powders was calculated [12].

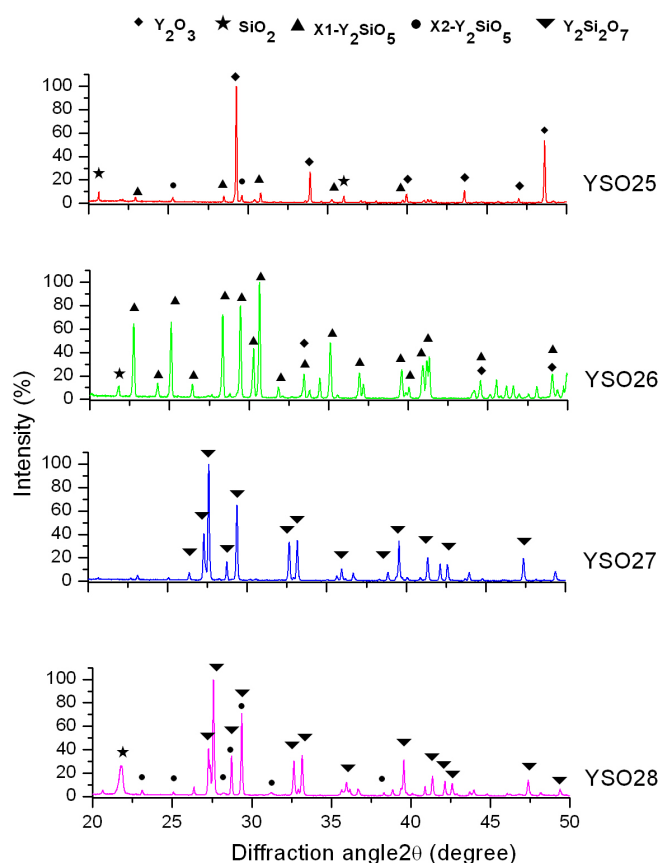


Figure 1. The X-ray diffraction patterns ($\lambda_{\text{Cu}}=1.540598\text{\AA}$) of samples prepared with different $\text{MR}_{\text{Si:Y}}$

Composition of the starting synthesis mixtures together with some microstructural parameters are presented in Table 1.

When yttrium oxide is used in excess (the case of $\text{MR}_{\text{Si:Y}}=1:4$, sample YSO25), the synthesis mixture contains mainly un-reacted crystalline cubic yttrium oxide phase in proportion of 89.4 vol.% together with 2 vol.% of unreacted tetragonal silicon dioxide and 8.6 vol.% X1, X2 yttrium silicate. When stoichiometric amounts of yttrium oxide and silica oxide were used in

sample YSO26, the phase $X2-Y_2SiO_5$ becomes the dominant (81.7 vol.%). Excess of silica dioxide ($MR_{Si:Y} = 1:0.5$) in the synthesis mixture leads to the formation of one phase powder that consists only in monoclinic yttrium disilicate- $Y_2Si_2O_7$.

The results are in agreement with the literature data namely: Y_2O_3 -cubic phase (PDF 43-1036); SiO_2 tetragonal phase (PDF 39-1425); $X1-Y_2SiO_5$ monoclinic phase, (PDF 41-0004); $X2-Y_2SiO_5$ monoclinic phase (PDF 21-1458) and $Y_2Si_2O_7$ monoclinic phase (PDF 38-0440).

Table 1. Microstructural parameters for $SiO_2 - Y_2O_3$ based phosphors

Sample	$MR_{Si:Y}$	Microstructural parameters				
		Phase	$a[\text{\AA}]$	$b[\text{\AA}]$	$c[\text{\AA}]$	$V[\text{\AA}^3]$
YSO25	1:4	Y_2O_3 -cubic(89.4%)	10.616	10.616	10.616	90.0 1189.0
		$X1-Y_2SiO_5$ (8.4%)	8.400	6.841	6.383	103.0 357.5
		$X2-Y_2SiO_5$ (0.2%)	10.317	6.623	12.583	103.7 835.1
		SiO_2 tetragonal (2 %)	4.973	4.973	6.923	90.0 171.2
YSO26	1:1	Y_2O_3 -cubic (8.3%)	10.507	10.507	10.507	90.0 1159.9
		$X2-Y_2SiO_5$ (81.7 %)	10.420	6.726	12.499	102.6 854.9
		SiO_2 tetragonal (10.0%)	4.973	4.973	6.923	90.0 171.2
YSO27	1:0.5	$Y_2Si_2O_7$ -monoclinic 100%	6.871	8.968	4.718	101.7 284.7
		$Y_2Si_2O_7$ (78.8%)	6.871	8.969	4.719	101.7 284.8
YSO28	1:0.25	$X2-Y_2SiO_5$ (6.2%)	10.453	6.732	12.444	103.0 854.0
		SiO_2 tetragonal (15.0%)	4.973	4.973	6.923	90.0 171.2

FT-IR spectra for yttrium silicate based samples are presented in Figure 2. Significant changes are observed as the amount of SiO_2 increases from 20 mol.% to 80 mol.%, in the synthesis mixture.

The vibrational bands in FT-IR spectra in $400-1400\text{ cm}^{-1}$ domain can be grouped in three main regions namely:

- $1070-1200\text{ cm}^{-1}$ domain for stretching vibrations of silicon atoms against oxygen atoms in Si-O-Si bonds in $\beta-Y_2Si_2O_7$ phase [13];
- $850-1000\text{ cm}^{-1}$ domain corresponds to Si-O stretching vibration involving non-bridging oxygen. The band situated at around 849 cm^{-1} is ascribed to multiple Si-O stretching in which all oxygen and silicon atoms of silicate groups participate in the vibration [13];
- $400-600\text{ cm}^{-1}$ domain consist in lower vibrational bands more difficult to characterize, because single Y-O and Si-O vibrations coexist in similar spectral ranges. It can be stated that the vibrations situated in the range $600\text{ to }500\text{ cm}^{-1}$ are mainly due to Y-O stretching, and those from $500\text{ to }400\text{ cm}^{-1}$ are vibrations with a large component of Si-O bending [14,15].

It can be seen that as the SiO_2 amount decreases, the specific vibration for Si-O-Si bond in $\text{Y}_2\text{Si}_2\text{O}_7$ phase disappears (sample YSO27, YSO28) and bands from asymmetric stretching vibration in SiO_4^{2-} groups arise and become more structured (sample YSO25, YSO26).

Photoluminescence of Y_2SiO_5 : Ce phosphor samples was evaluated on the basis of excitation (PLE) and emission (PL) spectra and compared with an internal standard where the $\text{MR}_{\text{Si:Y}} = 1:1$. The internal standard was prepared by wet chemical synthesis route, using the SimAdd technique [16-18]. The intensity of the internal standard (YSO1.1) was considered to possess 100% photoluminescence [18].

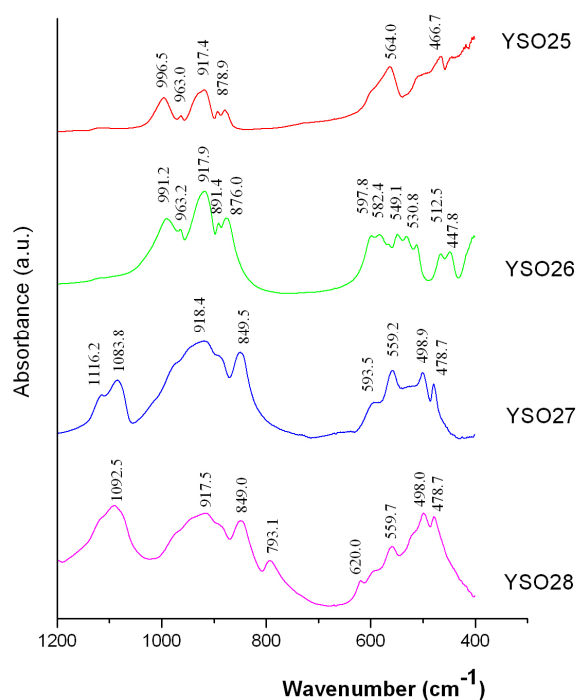


Figure 2. The FT-IR spectra of samples prepared with different $\text{RM}_{\text{Si:Y}}$

Figure 3 and Figure 4 show the PLE and PL spectra of Ce^{3+} activated Y_2SiO_5 samples synthesized by solid state reaction with different SiO_2 : Y_2O_3 molar ratio.

The excitation spectra can give also information on the nature of the luminescent centres.

In this respect, the excitation spectra taken in the range of 220–400 nm present three wide bands (Figure 3). These bands (designated with I, II, III) are associated with the crystal field split of Ce^{3+} 5d electronic levels.

The excitation peaks of the internal standard (sample YSO 1.1) are situated at 265 nm, 300 nm and 356 nm, respectively.

The intensity and the position of excitation peaks of the yttrium silicate samples are variable and depend on the $\text{SiO}_2\text{:Y}_2\text{O}_3$ molar ratio. For samples YSO30 and YSO32, the peaks I and III present a shift from 265 nm to 246 nm and from 356 nm to 349 nm, respectively.

The excitation spectra for samples prepared with excess of SiO_2 namely YSO30 ($\text{MR}_{\text{Si:Y}}=1:0.25$) and YSO32 ($\text{MR}_{\text{Si:Y}}=1:0.5$) present a similar behaviour. Thus, the peak II with maximum situated at 301 nm for samples YSO30, YSO32 is more broad compared to the corresponding one situated at 299 nm for sample YSO29 and 300 nm for standard.

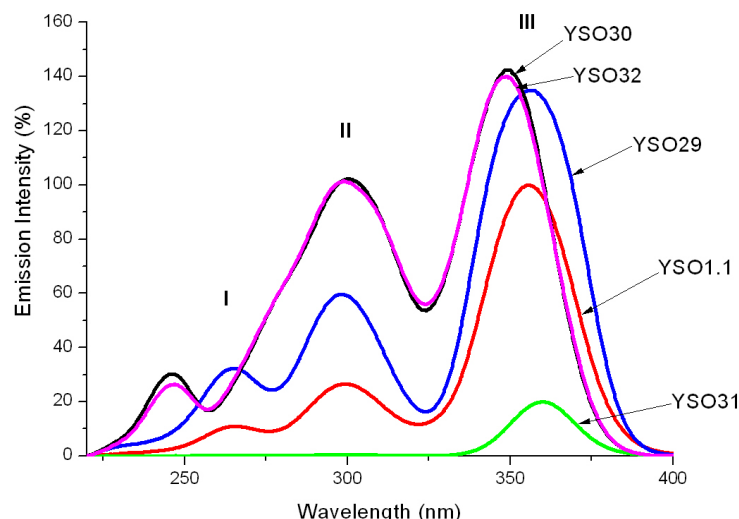


Figure 3. Excitation spectra of some YSO samples ($\lambda_{\text{em}}=420\text{nm}$)

The photoluminescent characteristics correlated with XRD and FT-IR data, lead to the conclusion that depending on the molar ratio, different luminescent centres are formed. In samples YSO30 and YSO32, the Ce^{3+} surrounding is given by the presence of the $\text{Y}_2\text{Si}_2\text{O}_7$ as host lattice, meanwhile in sample YSO 29 the luminescent centers are formed in an Y_2SiO_5 host lattice.

Excitation spectrum of the sample YSO31, prepared with $\text{SiO}_2\text{:Y}_2\text{O}_3$ molar ratio of 1:4, presents only one broad band with low intensity with a maximum situated at 361 nm. The reduced excitability of YSO31 sample can be also explained in correlation with XRD data. Due to the formation of a non-homogeneous powder that consists mainly in a mixture of unreacted Y_2O_3 and SiO_2 together with Y_2SiO_5 in relative small proportion, the incorporation degree of cerium is reduced.

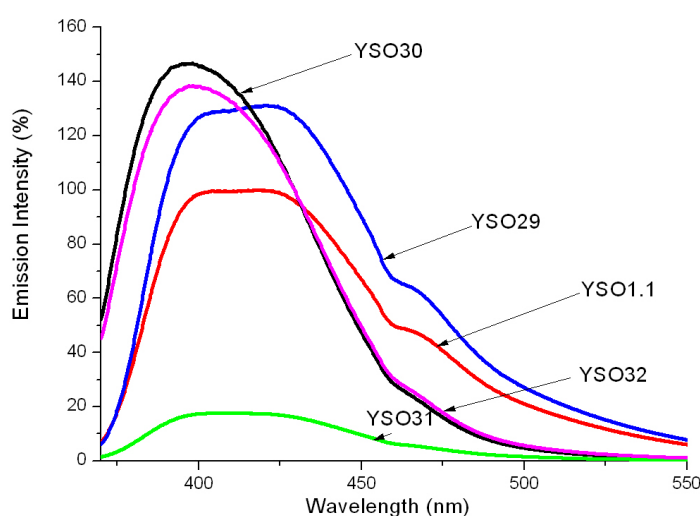


Figure 4. Emission spectra of some YSO samples ($\lambda_{\text{ex}}=356\text{nm}$)

Under UV light (365 nm) all YSO samples exhibit a luminescent emission situated in the blue domain of visible spectra. The emission spectra present a wide band with a maximum situated at around 400 nm as a result of the $4f$ energy levels splitting into $4f_{5/2}$ and $4f_{7/2}$ in cerium activator (Figure 4).

The Ce^{3+} activator ($r_{\text{Ce}^{3+}} = 0.106 \text{ nm}$) can easily substitute Y^{3+} from the oxide host lattice ($r_{\text{Y}^{3+}} = 0.104 \text{ nm}$) and populate two crystallographic sites in $\text{X1-Y}_2\text{SiO}_5$ and $\text{X2-Y}_2\text{SiO}_5$. If there is an excess of SiO_2 , the chemical surrounding of the Ce^{3+} becomes more complicated due to the formation of $\text{Y}_2\text{Si}_2\text{O}_7$ with different structures [11].

A double broad emission band with peaks situated at around 402 nm and 423 nm respectively, due to the splitting of the $4f^1$ ground configuration of the cerium ions into $^2F_{5/2}$ and $^2F_{7/2}$ can be observed for both YSO1.1 (standard) and YSO29 sample.

Considering the XRD information for $MR_{Si:Y}=1:1$ we can assume that the luminescent centres in sample YSO29 are given mainly by the presence of Ce^{3+} activators in $X2-Y_2SiO_5$ host lattice.

The emission intensity and the peak positions are modified as the composition of the silicate based samples is changed. Sample prepared with excess of silicon dioxide posses similar emission curves as can be observed for samples YSO 30 and YSO32 in which the main component is $Y_2Si_2O_7$. This samples have high photoluminescence ($I_{em} = 147\%$ and $I_{em} = 137\%$) with the maximum situated at 398 nm

Another tendency easily observed in the emission spectra is the large emission tail which extends toward the red region of the visible spectrum (from 450 to 550 nm) as well as the shoulder situated at 465 nm. This behaviour is associated with 5d-4f transitions and the formation of Y_2SiO_5 phase [19].

CONCLUSIONS

Yttrium silicate based materials were prepared by solid state reaction with different $SiO_2:Y_2O_3$ molar ratios in order to study the influence of the synthesis mixture composition on the structural and luminescent properties. It was revealed that $MR_{Si:Y}$ influences the structural and luminescent characteristics of samples.

The XRD patterns and FT-IR spectra put in evidence that the phosphor samples are formed from a mixture of unreacted Y_2O_3 and SiO_2 together with monoclinic $X1-Y_2SiO_5$, $X2-Y_2SiO_5$ and $Y_2Si_2O_7$ phases in various proportions depending on the molar ratio.

The photoluminescent investigations put in evidence that under UV light all yttrium silicate based samples exhibit more or less intense blue emission. The excitation spectra have three broad bands which present a shift toward shorter wavelengths as the content of the SiO_2 increase. The excess of Y_2O_3 leads to samples with small excitability and low emission intensity. This suggests that an insufficient amount of SiO_2 can not assure the formation of the proper host lattice surroundings for Ce^{3+} . An excess of SiO_2 in the synthesis mixture generates the formation of monoclinic yttrium disilicate phase with a high luminescent emission.

EXPERIMENTAL SECTION

Two samples series of yttrium based silicate powders were prepared by solid-state reaction method. In this respect, homogeneous synthesis mixtures containing Y_2O_3 (Sigma Aldrich) and SiO_2 (Sigma Aldrich) as generator of host-lattice and $Ce(NO_3)_3 \cdot 5H_2O$ (Sigma Aldrich) as activator supplier were fired at high temperature ($1400^\circ C$) for 4 hours, in air, using alumina crucibles. The yttrium silicate based powders were carefully washed, dried and sieved.

The first sample series is formed from samples: YSO25, YSO26, YSO27 and YSO28 which are prepared using different $\text{SiO}_2\text{:Y}_2\text{O}_3$ molar ratios namely: 1:4, 1:1, 1:0.5 and 1:0.25 respectively.

Second set of samples consist of samples: YSO29, YSO30 YSO31, YSO32 which are prepared using different $\text{SiO}_2\text{:Y}_2\text{O}_3$ molar ratios namely: 1:1, 1:0.25, 1:4, 1:0.5 and are prepared using 3% mol Ce /(Y+Ce) in the synthesis mixture in order to generate photoluminescent properties. The internal standard (YSO1.1) was prepared by SimAdd method using ammonium oxalate (Merck 99.9%), yttrium oxide (Aldrich 99.99%), cerium nitrate (Merck, extra pure) and silicagel powder (Alfa Aesar) as starting materials [16-18]. The synthesis consist in the thermal treatment at 1600°C in nitrogen for 4 hrs of the precursor prepared by precipitation of yttrium-cerium nitrate solution, with ammonium oxalate solutions and silica suspension at pH=6 [18]. The post-precipitation stage consisted of 24 h aging, centrifuge separation, water wash and drying.

Samples were characterised by photoluminescence spectroscopy, X-ray diffraction (XRD), infrared absorption spectroscopy (FT-IR). The emission (PL) and excitation (PLE) spectra were registered with JASCO FP-6500 Spectrofluorimeter Wavel (Farbglassfilter WG 320/ Reichmann Feinoptik-Ger). X-ray diffraction patterns were obtained with BRUKER X8 ADVANCE X-Ray Diffractometer ($\text{CuK}\alpha$ $\lambda=1.540598\text{\AA}$ radiation). The infrared absorption spectra were measured with a NICOLET 6700 Spectrometer (KBr pellets technique).

ACKNOWLEDGMENTS

Financial support for this study was provided by the Romanian Ministry of Education, Research and Innovation (Project 71-122).

REFERENCES

1. W.M. Yen, S.Shionoya, H. Yamamoto, "Practical application of phosphors", CRC press, Taylor & Francis Grup, Boca Roton-London-New York, **2007**.
2. R.Y. Lee, F.I. Zhang, *J. Vac. Sci. Technol.*, **1998**, B16, 1013.
3. M. Leskelaa, *J. Alloys Compd.*, **1998**, 275-277, 702.
4. H. Jiao, X. Wang, S. Ye, *J. Lumin.*, **2007**, 122-123, 113.
5. X. Qin, Y. Ju, S. Bernhard, Nan Yao, *Mater. Res. Bul.*, **2007**, 42, 1440.
6. H. Jiao, L. Wei, N. Zhang, M. Zhong, X. Jing, *J. Eur. Ceramic Soc.*, **2007**, 27, 185.

7. E.M. Levin, C.R. Robbins, H.F. McMurdie, Phase Diagram for Ceramists, Fig. 2388, in M.K. Reser (Ed.), American Ceramic Society, Columbus, OH USA, **1969**.
8. Q.Y. Zhang, K. Pita, *J. Phys. D. Appl. Phys.*, **2002**, 35, 3085.
9. C. Michel, G. Buisson, E.F. Bertaut, *C.R. Acad. Sci. B*, **1967**, 264, 397.
10. N. I. Leonyuk, E. L. Belokoneva, G. Bocelli, L. Righi, E. V. Shvanskii, R. V. Henrykhson, N. V. Kulman, D. E. Kozhbakhteeva, *Cryst. Res. Technol.*, **1999**, 34, 1175.
11. J. Felsche, *Struct. Bond.*, **1973**, 13, 99.
12. W. Kraus, G. Nolze, *J. Appl. Crystallogr.*, **1996**, 29, 301.
13. M. Di'az, C. Pecharra'm'a'n, *Chem. Mater.*, **2005**, 17, 1774.
14. Y. Repelin, C. Proust, E. Husson, J. M. Beny, *J. Solid State Chem.*, **1995**, 118, 163.
15. A. M. Hofmeister, A. Chopelas, *Phys. Chem. Miner.*, **1991**, 17, 503.
16. E.J. Popovici, L. Muresan, A. Hristea, E. Indrea, M. Vasilescu, *J. Alloys Compd.*, **2007**, 434-435, 809.
17. L. Muresan, E.J. Popovici, R. Grecu and L. Barbu Tudoran, *J. Alloys Compd.*, **2009**, 471, 421.
18. L. Muresan, M. Stefan, E. Bica, M. Morar, E. Indrea, E.J. Popovici, *J. Optoelectron. Adv. M. - Symposia*, **2010**, 2, 131.
19. J.A. Gonzalez-Ortega, E.M. Tejada, N. Perea, *Opt. Mater.*, **2005**, 27, 1221.